Environmental Engineering and Management Journal

February 2015, Vol.14, No. 2, 389-397
http://omicron.ch.tuiasi.ro/EEMJ/

"Gheorghe Asachi" Technical University of Iasi, Romania

NEW COMPLEXES OF 2-(1H-1, 2, 4-TRIAZOL-3-YL) PYRIDINE WITH Co(II), Cd(II), Rh(III), IONS: SYNTHESIS, STRUCTURE, PROPERTIES AND POTENTIAL APPLICATIONS

Petronela Horlescu[1], Daniel Sutiman[1], Corneliu S. Stan[1*], Carmen Mita[2], Cristian Peptu[3], Maria E. Fortuna[3], Cristina Albu[1]

[1] *"Gheorghe Asachi" Technical University of Iasi, Faculty of Chemical Engineering and Environmental Protection, 73 Prof. Dr. docent Dimitrie Mangeron Str., 700050 Iasi, Romania*
[2] *"Alexandru Ioan Cuza" University of Iasi, Faculty of Chemistry, 11 Carol I Blvd., 700506 Iasi, Romania*
[3] *"Petru Poni" Institute of Macromolecular Chemistry, 41A Grigore Ghica Voda Alley, 700487 Iasi, Romania*

Abstract

Co(II), Cd(II) and Rh(III) complexes with 2-(1H-1,2,4-triazol-3-yl)pyridine (Htzp) as ligand were synthesized and investigated. The neutral mononuclear complexes with a generic [M(tzp)n] structure have been prepared from Htzp and corresponding transition metals chlorides at 2:1 and 3:1, respectively molar ratios in H_2O–EtOH. The resulted crystalline complexes were investigated through magnetic and molar conductivity measurements, elemental analysis, FT-IR, mass spectroscopy, thermal analysis, UV-Vis and P-XRD. The experiments indicate that Htzp acts as bidentate anionic ligand, $[Co(tzp)2]\cdot 1.5H_2O$ and $[Cd(tzp)_2]$ are in the tetragonal coordination, whereas six coordinate octahedral $[Rh(tzp)_3]\cdot H_2O$ complex undergoes a weak tetragonal distortion. In case of Co(II) complex, an interesting feature was revealed through fluorescence spectroscopy, as the fluorescent emission intensity of the free ligand is dependent on the Co(II) solution content. Through complexation, the fluorescence is gradually quenched according to the Co(II) aqueous solution content, which may recommend it as a method of detection of Co(II) presence in waste water.

Key words: Co(II) detection, ligand, transition metal complexes, triazole complexes

Received: November, 2014; Revised final: February, 2015; Accepted: February, 2015

1. Introduction

Heterocyclic chemistry has now become a separate field of inorganic chemistry with long history, present society and future prospect (Yousif et al., 2013). In recent years, studies on complexes with N containing ligands have attracted considerable interest due to their important role in the development of coordination chemistry as well as inorganic biochemistry, catalysis and optical and magnetic materials.

Triazole classes are considered to be excellent coordinating ligands, because they involved both hard nitrogen and amino group. Furthermore, compounds containing the nucleus triazole and the pyridine are part of an increased interest from the researchers due their multiple chemical, biological and medical applications, through the chromophore properties (colorants) (Haasnoot, 2000), luminescent (Inkaya et al., 2013; Shan et al., 2013; Shang et al., 2013), catalytic (Bortoluzzi et al., 2013), bacterial activities (Crabtree, 2001; Meek et al., 2011; Liu et al., 2011; Stock and Biswas, 2012), antifungals (Dong et al., 2010; Werner and Stiasny, 1899), antivirals (Chen et al., 2011), antidepressants (Wilson and Wilson, 1955), asthmatics (Meunier et al., 1976) and inflammatory (Bladin, 2006; Potts, 1961). Also, a significant number of compounds were considered,

* Author to whom all correspondence should be addressed: e-mail: stcornel@gmail.com; Phone: 0742208215

because they have antidiabetic (Ding et al., 2005) and diuretics properties (Zhang and Chen, 2006). The organic compound 1, 2, 4 – triazole-3-one, derived from the 1,2,4 – triazole, is particularly interesting due its, antitumor and antibacterial properties. 1,2,4-triazole and 1,2,4-triazol-3-one are important heterocycles being incorporated into a wide variety of drugs like Fluconazole, Itraconazole, Voriconazole, Posaconazole, Letrozole, and Anastrazole used in medical therapy (Pardeshi and Bobade, 2011). Tabatabaee et al. (2012) reported the fact that 1,2,4 –triazoles function as ligands mono-, bi- or tridents, obtaining coordination compounds like the monomers class, dimers and polynuclear species. Reedijks et al. (2011) obtained a series of trinuclear compounds using derivatives from class 1, 2, 4 –triazoles with transition metals M= Mn, Fe, Co, Ni and Zn.

This study presents the synthesis and the structural characterization of new coordinative compounds of the Co(II), Rh(III) and Cd(II) cations with 2-(1H-1,2,4-triazol-3yl)pyridine, a derivative from 1,2,4 - triazoles class. The research was extended to the possibility of detection of Co(II) presence in water due to the observed fluorescence emission quenching of the free ligand through complexation. The Cd(II) complex is an interesting alternative to be used as precursor in CdSe Quantum Dots synthesis while the Rh(III) complex may be valued in catalytic processes where the presence of rhodium is required.

2. Experimental

2.1. Materials

$CdCl_2$ (99.9%), $CoCl_2 \cdot 6H_2O$ (99%) and $RhCl_3 \cdot xH_2O$ (99.98%) were purchased from Alfa-Aesar. 2 - (1H-1, 2, 4-triazol-3-yl) pyridine (Htzp) (97%) with the structure presented in Fig. 1 was purchased from Sigma-Aldrich. All the chemicals were of reagent grade and used as received. Solvents used in the synthesis procedure are absolute ethanol (Merck) and high purity MiliQ water.

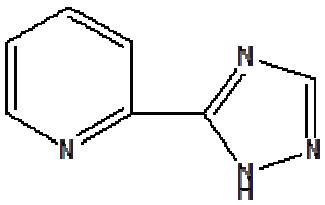

Fig. 1. The structure of 2-(1H-1, 2, 4-Triazol-3-yl) pyridine (Htzp)

2.2. Preparation

First, for the preparation of aqueous solutions of chlorides of Cd, Co and Rh was dissolved 1 mmol of each in 2 mL of double distilled water. The solutions of 2 - (1H-1, 2, 4-triazol-3-yl) pyridine were prepared by dissolving 3mmol of the ligand in a mixture of 3 mL of water and 1 mL of ethanol. The complexes were prepared by mixing of ligand solution with chloride solution of Cd^{2+}, Co^{2+}, Rh^{3+}, respectively. The complexation reactions (Eq. 1) were carried out under heating (40-45^0 C) and stirred for 180 minutes. All complexes were obtained by the reaction of M and Htzp in the 1:2 molar ratio for Co, Cd/Htzp and 1:3 molar ratio for Y, Rh/Htzp.

$$MCl_n + nHtzp = [M(Htzp)_n] + nHCl \uparrow \quad (1)$$

where: M= Co, Cd, n=2; M= Rh, n=3.

The crystalline complexes were separated by filtration and then washed with double distilled water. The obtained compounds were purified by re-crystallization from the ethanol solution. The traces of solvent were removed by drying in the vacuum at room temperature.

2.3. Methods

Elemental analysis was performed with the Thermo Fischer Scientific device Flash EA-1112CHNS/O equipment supplied with the software Eager 300. Metal elemental chemical analysis was performed by atomic absorption. The thermal stability of the prepared complexes was analyzed by TG measurement on a Mettler Toledo TGA-SDTA851e device, under air flow of 20 ml / min, at a heating rate of 10 $K \cdot min^{-1}$. The kinetic parameters have been calculated by Coats-Redfern, Flynn Wall and Urbanovici Segal methods. The conductivity of $2 \cdot 10^{-4}$ M ethanolic solutions was determined with Consort K912 electrochemical analyzer at 25 ^{0}C. Magnetic properties of solid compounds were determinated with a magnetic Sherwood Scientific MS auto-balance by Gouy method at room temperature against $Hg[Co(SCN)_4]$ as standard.

IR spectra of the ligand and metal complexes were recorded using Digilab FTS-2000 FT-IR spectrophotometer, in the 4000-400 cm^{-1} range, according to KBr pellet method. The UV-VIS absorption spectra of solid samples were performed with CAMSPEC 501M single beam spectrophotometer provided with a diffuse reflectance sphere, using $BaSO_4$ as blank, in the 190–1100 nm range. The number and energy of transition bands were resolved by the deconvolution of the original electronic diffuse reflectance spectra (DRS) using OrigineLab programs. XRD patterns were recorded in the 5-70^0 2Theta range on a Panalytical X 'Pert Pro diffractometer equipped with a Cu-Kα radiation source (λ = 0.154060 nm). Unit cell parameters of the investigated complexes were further refined using software Panalytical X 'Pert High Score Plus.

High-resolution MS and MS/MS spectra were acquired on an AGILENT 6520 QTOF mass spectrometer equipped with an ESI source. The ESI MS parameters optimized for the analyzed complexes were set as follows: Vcap = 4000 V,

fragmentor voltage = 175 V, drying gas temperature = 325 ^{o}C, drying gas flow = 5 L/min and nebulizer pressure = 35 psig. Nitrogen was used as spraying gas. On this instrument, the MS/MS experiments were conducted in the collision cell using nitrogen as collision gas at a pressure of 18 psig inside the collision cell. The steady state fluorescence spectra were recorded on a Horiba Fluoromax 4P spectroflurometer.

3. Results and discussion

3.1. Elemental analysis

The results of elemental analysis recorded for $[Co(Htzp)_2]$ (**1**), $[Cd(Htzp)_2]$ (**2**) and $[Rh(Htzp)_3]$ (**3**) are presented in Table 1. The elemental analysis data were correlated with those obtained by thermogravimetric analysis.

3.2. FT-IR analysis

The infrared spectrum of **Htzp** (Fig. 2) shows in the 3350 – 2700 cm^{-1} range an intense broad band structured in five components assigned to ν(NH)triazole and ν(CH)pyridine/triazole. The ν(NH) stretching vibration is observed at 3082 cm^{-1} and 3151 cm^{-1}. The shoulder can be attributed to N-H···N intermolecular hydrogen bond. The ν(CH)pyridine stretching vibrations are observed at 2936 and 2866 cm^{-1}, while ν(CH)triazole vibration is located at 2801 cm^{-1} due to the lower bond order of C-H triazole group. A series of very weak intensity bands were recorded in the 2800 - 1800 cm^{-1} range which can be attributed to the combined bands of deformation vibration by Fermi resonance (Nakamoto, 1997).

The medium peak centered at 1597 cm^{-1} was attributed to the ν(C=N) pyridine stretching vibration, but the wider bandwidth can be due to overlapping of ν(C=N)pyridine stretching mode and ν(C=C)pyridine vibration. The ν(C=N)triaziole stretching vibration is characterized by a strong sharp band located at 1477 cm^{-1}. The band observed at 1404 cm^{-1}, which can be attributed to the ν(C-N)triazol stretching modes, is partial overlapped with γ(N-H)triazole + γ(C-H)pyridine rocking vibration modes. The C-C, C-N pyridine and N-N pirazole stretching vibrations in broad bands of 1300 – 1000 cm $^{-1}$ range are complicated and mixed with other vibrational modes.

The FTIR spectra of **1** and **3** presents in the 3500 – 3200 cm^{-1} range two bands centered at 3415 cm^{-1} and 3431 cm^{-1}, respectively, due to asymmetric and symmetric ν(OH) stretching vibration modes of water. The intensity and broadness of these bands suggest that the water molecules are not coordinated at metal cations but can be involved in the hydrogen bonds with the one of nitrogen atoms of triazole ring. The asymmetric and symmetric ν(OH) stretching vibration modes of water is not present in the infrared spectrum of Cd(II) complex (**2**). After coordination of **Htzp** to metal cation the ν(N-H)triazole can not be identified. This is in agreement with the UV-Vis and conductance results. Modification of charge density from pyridine and triazole rings determined the shifting of C-H, C=C, C=N and N-N stretching vibration modes. The ν(C-H)pyridine and ν(C-H)triazole generate two separated relatively broad bands centered at 3074 and 2882 cm^{-1} (for **1**), 3072 and 2887 cm^{-1} (for **2**), 3084 and 2889 cm^{-1} (for **3**), respectively.

The hipsochromic shift of ν(C-H) indicates the increasing of the covalent character of C-H bonds as a consequence of the decreasing of electronic density on the carbon atoms. The relative high intensity of ν(CH) frequency bands of **3** exceed the intensities of the other IR bands, the position and intensity of the bands being dependent by the vibration modes of tzp^{-} ligand, strongly coupled with other skeletal modes. This could be due to the simultaneous increasing of polarities of both type of C-H bonds (pyridine and triazole) and the steric hindrance of coordinated ligand (Bellagamba et al., 2013). In the 1700 – 1000 cm^{-1} range the spectra of all complexes revealed the relatively broad bands of free Htzp becoming more intense and sharp after tzp^{-} coordination to metal center.

The process is accompanied by the shift of the ν(C=N)pyridine (1612 cm $^{-1}$ for **1** and **3**, 1660 cm^{-1} for **2**) and ν(C=N)triaziole (1495 cm^{-1} for **1**, 1550, 1478 cm^{-1} for **2**) to higher energy, excepting ν(C=N)triaziole of **3** (1466 cm^{-1}), due to the increasing of the C=N bonds, order which is determined by the electrophilic effect of the metal cation. Splitting of frequency of triazole C=N bonds suggest that the Cd(II) cation interacts more with the N atom, derived from the HN group, than the N atom of pyridine. The decrease of electronic density of coordinated nitrogen atom is compensated by decreasing of negative charge density on the nearest atom with low electronegativity. The same effect was observed for the (C-N) triazole and (N-N) triazole: wavenumbers increase from 1404 cm^{-1} (**Htzp**) to 1427 (**1**) and 1419 cm^{-1} (**2** and **3**) for ν(C-N) triazole and from 1269 cm^{-1} (**Htzp**) to 1271 (**1**), 1273 (**2**), 1288 and 1257 cm^{-1} (**3**) for ν(N-N) triazole. In case of rhodium complex (**3**), the splitting of ν(N-N)triazole band could be due to the Jahn-Teler effect on one direction (equatorial or axial), the steric hindrance and/or influence of the crystalline lattice by symmetry group and formation of a hydrogen bonding between water molecule and a nitrogen atom of one tzp^{-} ligand.

The corresponding deformation band, assigned of $\delta(H_2O)$ is overlapped by the strong ν(C=N)pyridine bands. In the 700 – 400 cm^{-1} range were identified by the deconvolution of original **1, 2** and **3** spectra, four bands assigned to symmetric and asymmetric ν(M-N) vibrations at 636, 543, 484 and 462 cm^{-1} for **1**; 683, 476 and 412 cm^{-1} for **2**; 665, 631, 513 and 459 cm^{-1} for **3**. These indicate the nonequivalence of the M-N bonds, the high energy vibration being a quantitative parameter of M-N triazole bond strength: Cd^{2+}-N > Rh^{3+}-N > Co^{2+}-N. The position and intensity of ν(M-N) bands are

dependent by the stereochemical configuration of complexes, vibration modes of ligand being strongly coupled with other skeletal modes. As expected from symmetry consideration, the cis-isomer will exhibit two ν(M-Npyridine) and ν(M-Ntriazole) modes whereas the trans-isomer only one for each type of these modes. The all complexes exhibit both types of stretching vibrations, but the symmetry of Cd^{2+} coordination center is higher than of Co^{2+} and Rh^{3+} complexes (Zhang and Zhang, 2013).

3.3. Mass spectroscopy

The $[Co(tzp)_2(H_2O)_{1.5}]$ complex was analyzed through ESI mass spectrometry. The obtained spectrum is showed in the Fig. 3A. The peak observed at m/z = 495 was associated with the presence of a complex of Co with three ligand molecules [495 = 59 (Co) + 145 (L)x3 + 1(H)]

Also, there may be observed a second peak with higher intensity, at m/z = 350 corresponding to the complex of Co with two ligand molecules. This peak is probably formed in ESI MS conditions through the loss of a ligand molecule and represents a more stable form in electrospray conditions. Nevertheless, the performed experiment allows the qualitative identification of the $[Co(tzp)_2(H_2O)_{1.5}]$ complex.

Table 1. Theoretical and experimental chemical composition of synthesized compounds

Compound	*Experimental (calculated) mass, %*					*Molecular weight, g/mol*	*Empirical/ molecular formula*
	C	*N*	*O*	*H*	*M*		
1	43.98 (44.64)	29.30 (29.76)	6.55 (6.37)	3.88 (3.98)	15.85 (15.67)	376.28	$Co^{2+}C_{14}H_{15}N_8O_{1.5}$ $[Co(tzp)_2].1.5H_2O$
2	41.86 (41.75)	28.22 (27.83)	- -	2.90 (2.98)	28.05 (27.83)	402.68	$Cd^{2+}C_{14}H_{12}N_8$ $[Cd(tzp)_2]$
3	44.57 (45.28)	29.77 (30.19)	2.95 (2.87)	3.77 (3.59)	18.23 (18.51)	556.42	$Rh^{3+}C_{21}H_{20}N_{12}O$ $[Rh(tzp)_3].H_2O$

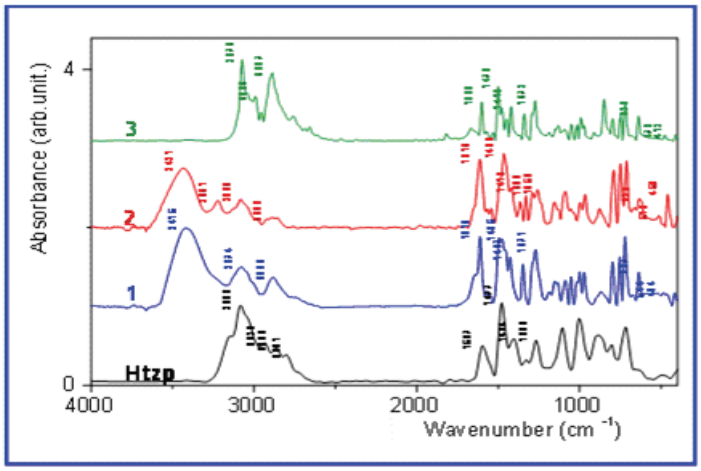

Fig. 2. FTIR spectra of Htzp, $[Co(tzp)_2]\cdot 1.5H_2O$ **- 1**, $[Cd(tzp)_2]$ **- 2** and $[Rh(tzp)_3]\cdot H_2O$ – **3**

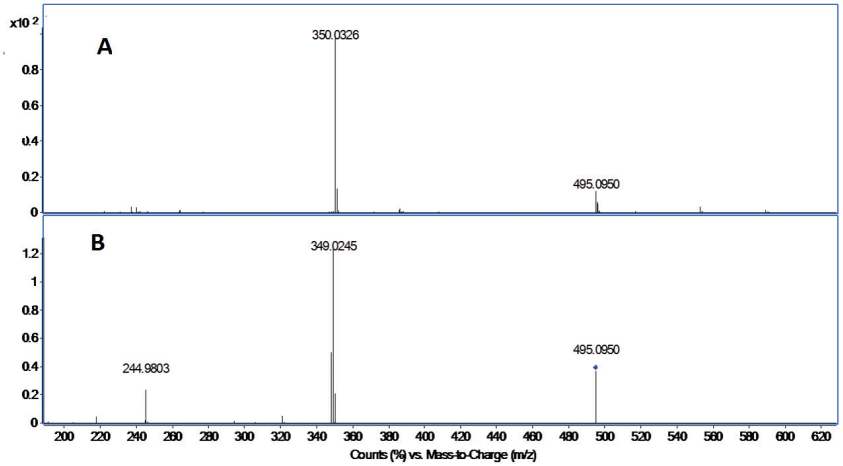

Fig. 3. A: ESI MS spectrum of $[Co(tzp)_2(H_2O)_{1.5}]$ complex; B: ESI MS/MS fragmentation of 495 peak

The fragmentation of the 495 peak in MS/MS conditions was attempted to further confirm the MS assignments. The MS/MS spectrum presented in figure 3B shows that the 495 peak losses one ligand molecule (146 m/z corresponds to the mass of the Htzp ligand) and leads to the formation of the ionic species with m/z = 349. A supplementary loss of m/z = 105 (peak found at m/z = 244) is related to further fragmentation of the ligand molecule as confirmed by the MS/MS fragmentation of the ligand molecule (spectra not given).

Overall, the ESI MS and MS/MS experiments confirm at molecular level the formation of the Co complexes with three ligand molecules.

3.4. DRS UV-Vis-NIR analysis

The spectra and values of band maxima for systems obtained are shown in Fig. 4 and Table 2. The DR spectra of all complexes show a number of partial overlapped intense bands in the 200 - 400 nm range (Fig. 4). After the original spectra deconvolution were identified 4 bands assigned to intraligand n-π* and π-π* transitions (Fig. 4, Table 2), which are dominated by the π-π* transitions of the pyridine and the triazol rings. Accordingly, in the electronic spectrum both energies of π_{py}-π* and π_{tz}-π* transitions upon coordination are shifted.

The values of energy decrease for the π_{py}-π* transition from 35336 cm^{-1} (**1**), 3464 cm^{-1} (**3**) to 34364 cm^{-1} (**2**) when the π_{tz}-π* transition is the same (41152 cm^{-1}) for **1** and **2** complexes. These suggest that the metal cations increase the electronic delocalization of ligand rings, more evident in case of Cd^{2+} complex.

The wavelengths of n-π* transition bands (Table 4) are also determined by the individual electronegativity of nitrogen atoms of – N=N- and – C=N- groups and the inductive electronic effect of metal cation. The shift of both n_N-π* transitions to lower energy, imply that the changes in the energy levels of the molecular orbitals of ligand upon coordination substantially originate from the increasing of polarizability of nitrogen atoms.

The electronic spectrum of **1** exhibits two intense bands at 10020 cm^{-1} and 20576 cm^{-1} due to d-d transitions. This pair of allowed electronic transitions can be generated by the distorted tetrahedral symmetry of coordination center by the nonequivalent donor atoms and steric hindrance. The tetrahedral Co^{2+}-d^7 high spin ground state is $^4A_2$. Three spin –allowed d-d transitions to the $^4T_2$, $^4T_1$and $^4T_1$(P) state is predicted but first transition lies at low energy (over detection limit of device).

The gap energy between the two transitions can allowed us to estimate that the tzp^- creates a relatively strong ligand field located at the boundary between ^4F (high spin) and ^2G (low spin) ground state. The Cd(II) – d^{10} configuration does not have the d-d transitions. In the spectrum of **3** were identified two d-d transitions. The energies and low intensities of absorption bands as well as the strength of ligand field (as **1**) are specific for the low spin Rh(III) - d^6 configuration in tetragonally distorted octahedra.

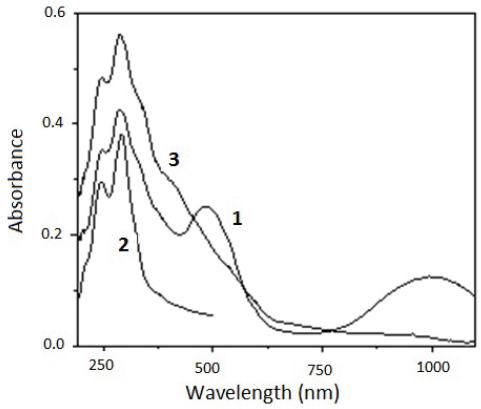

Fig. 4. The diffuse reflectance absorption spectra (DRS) of **1**- $[Co(tzp)_2]\cdot 1.5H_2O$, **2**- $[Cd(tzp)_2]$ and **3**- $[Rh(tzp)_3]\cdot H_2O$ complexes

Therefore, the two observed bands can be attributed to $^1E_g \leftarrow {}^1A_{1g}$ (19084 cm^{-1}) and $^1A_2 \leftarrow {}^1A_{1g}$ (22676 cm^{-1}) electronic transitions (Alasalvar et al., 2013). All three complexes exhibit in 26000 - 29000 cm^{-1} domain the charge transfer (CT) transitions (Table 4). The CT absorption bands are superposed with d-d (for **1** and **3**) and intra-ligand transitions. The intensity of CT are relatively high for $d(Co^{2+})$ - $\pi(tzp^-)$ and $d(Rh^{3+})$ - $\pi(tzp^-)$ transitions compared to $\pi^*(tzp^-)$-$d(Cd^{2+})$ (Fig. 4).

3.5. Electric conductance

The values of molar conductivity, Λ_M, of **1**, **2** and **3** (Table 3) are in agreement with their nature of nonelectrolytes. This behavior suggests the existence of anionic ligands in the coordination sphere which countervail the cation charge and also a relatively low polarization in electric field of the studied complexes.

3.6. Magnetic properties

The magnetic susceptibility values of **2** and **3** (Table 3) are characteristic to the class of diamagnetic compounds, while **1** belongs to paramagnetic class. With equation $\mu=2.84\cdot(\chi_M\cdot T)^{1/2}$ (χ_M – molar magnetic susceptibility, T – temperature, K) was calculated the effective magnetic moment for Co^{2+} complex as μ_{eff} = 0.92 μ_B. The μ_{eff} value for **1** and negative χ_{exp} of **3** could be explained by existence of a strong ligand field around Co^{2+} (d^7) and Rh^{3+} (d^6) cations.

3.7. P-XRD analysis

Calculated unit cell parameters of the Hpz free ligand and prepared complexes are presented in

Table 4. For exemplification, one of the recorded diffractograms (for the $[Cd(tzp)_2]$ complex) is presented in Fig. 5. The crystallization system is triclinic for the complexes while in case of free ligand, a monoclinic configuration was found.

3.8. Thermal analysis

Thermal analysis revealed significant differences in the decomposition schemes of the free ligand compared with the prepared complexes (Fig. 6 a-d). Thus, in the case of complexes four decomposition stages were recorded while in case of the free ligand only two decomposition stages were noted. Table 5 summarizes the parameters for each decomposition stage recorded for the free ligand and prepared complexes.

In the first stage, the remnant small amounts of physical bonded water and also the coordinated water is lost. In the second stage, the percent of mass losses suggests the breaking of the covalent C-C bond between the two constituent rings of the ligand (Fig. 1) and the elimination of the pyridine ring. This conclusion is sustained by the results recorded from mass spectroscopy investigation which also suggests the fragmentation of the ligand. In the upper stages the decomposition processes evolves with further destructuration of the complexes accompanied by volatile exhaustions. In each case, the recorded residual mass suggests the presence of Co, Rh, Cd oxides as final decomposition product along with small amounts of residue resulted from decomposition of the ligand (Mészáros et al., 1998; Sasidharan et al., 2011).

Table 2. The electronic spectral data (λ, cm^{-1}) of **1**- $[Co(tzp)_2]\cdot 1.5H_2O$, **2**-$[Cd(tzp)_2]$. and **3**- $[Rh(tzp)_3]\cdot H_2O$

Compound	*Transition*						
	Intra-ligand, (cm^{-1})				*Charge transfer (cm^{-1})*	*d-d, (cm^{-1})*	
1	51546	41152	35336	30960	26954	20576	10020
2	48309	41152	34364	30864	28329	-	-
3	46729	41322	34722	29940	26316	22676	19084

Table 3. The experimental magnetic susceptibility (χ_{exp}) and molar conductivity (Λ_M) of the prepared complexes

Compound		*Color*	Λ_M, $\Omega^{-1}.cm^2.mol^{-1}$	$\chi_{exp}.10^6$
1	$[Co(tzp)_2].1.5H_2O$	red-orange	35.711	0.319
2	$[Cd(tzp)_2]$	white	69.021	-6.057
3	$[Rh(tzp)_3].H_2O$	orange	40.991	-2.065

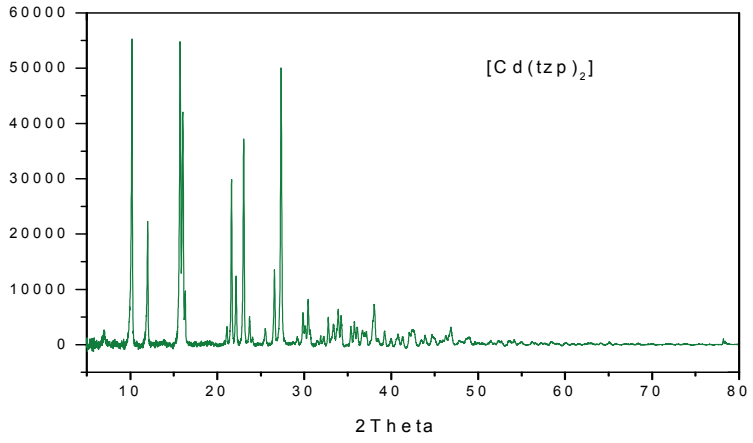

Fig. 5. Diffractogram recorded for the $[Cd(tzp)_2]$ complex

Table 4. Calculated unit cell parameters of the ligand and prepared complexes

Parameters	*Htzp*	*$[Co(tzp)_2]\cdot 1.5\ H_2O$*	*$[Rh(tzp)_3]\cdot H_2O$*	*$[Cd(tzp)_2]$*
a [Å]	10.53	5.5	4.672	6.801
b [Å]	3.96	10.5	10.83	15.92
c [Å]	8.90	16.5	10.95	15.28
Alpha [º]	90	38.35	88.6	47.1
Beta [º]	110.7	95.7	83.9	80.15
Gamma [º]	90	89.0	94.58	53.23
Volume [Å]	347.15	578.04	548.85	887.68
System	monoclinic	triclinic	triclinic	triclinic

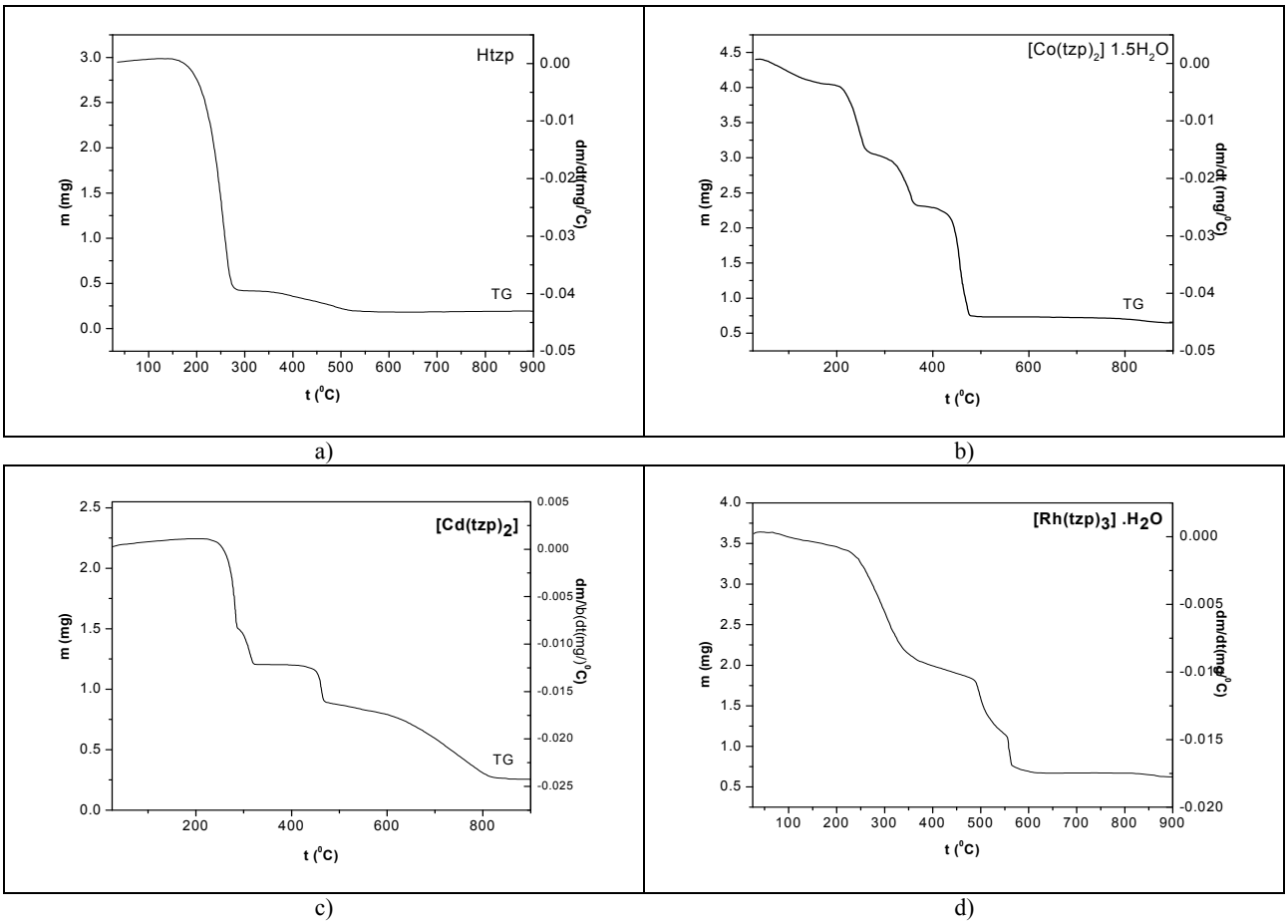

Fig. 6. Thermal analysis curves (TG) of the a) ligand Htzp and complexes b) $[Co(tzp)_2]\cdot 1.5H_2O$, c) $[Cd(tzp)_2]$, d) $[Rh(tzp)_3\cdot H2O]$

Table 5. Thermal decomposition stages, reaction order and activation energies (kJ/mol) of the ligand and prepared complexes

Decomposition Stage	***Parameter***	***Ligand***	***[Co(tzp)2.1.5(H2O)]***	***[Cd(tzp)2]***	***[Rh(tzp)2].H2O***
Stage 1	A	$1.62\cdot10^{18}$	1.49	$1.36\cdot10^{26}$	$0.51\cdot10^{2}$
	Ea/kJ/mol	74.05	18.48	295.01	28.70
	N	0.33	0.57	0.26	0.84
	Ti-Tf	203-272	56-146	253-280	75.4-185
	%loss	88.1	8.00	32.54	5.19
Stage 2	A	$20.1\cdot10^{18}$	$3.29\cdot10^{7}$	$9.98\cdot10^{15}$	4.95
	Ea/kJ/mol	45.3	94.85	199.37	34.92
	N	0.55	0.44	0.34	0.37
	Ti-Tf	365-516	208.1-256	290.5-317	231.5-340
	%loss	7.93	23.76	12.64	41.67
Stage 3	A	-	$3.02\cdot10^{9}$	$1.59\cdot10^{62}$	$1.33\cdot10^{32}$
	Ea/kJ/mol	-	137.51	894.5	496.17
	N	-	0.27	0.58	1.47
	Ti-Tf	-	318.9-355	447.8-464	481.2-513.2
	%loss	-	16.76	13.90	22.48
Stage 4	A	-	$5.47\cdot10^{35}$	$5.09\cdot10^{24}$	$6.18\cdot10^{3}$
	Ea/kJ/mol	-	521.22	56.89	85.55
	N	-	2.05	0.33	0.34
	Ti-Tf	-	431.2-476	613.1-810	545.8-803.1
	%loss	-	35.28	23.32	13.16

3.9. Fluorecence spectroscopy

As stated above, the fluorescent emission intensity of the free ligand, in presence of incremental quantities of Co(II) cations present in an aqueous solution tend to gradually diminish towards total quenching of the radiative transitions. Fig. 7 presents the variation of the fluorescent emission intensities during the addition of increasing quantities of Co(II).

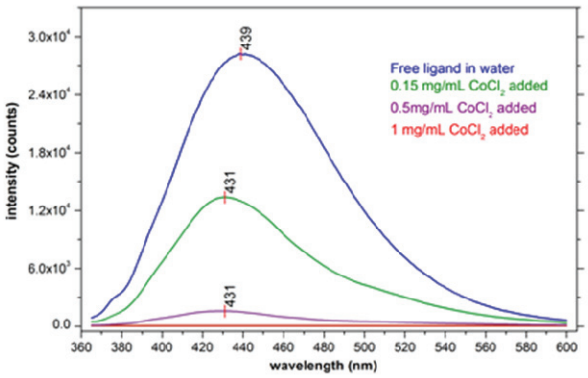

Fig. 7. Intensities of the fluorescence emission spectra recorded under 350 nm excitation for the free ligand and for increasing quantities of $CoCl_2$ added in the aqueous solution

During complexation, the presence of the central cation influence the excited states of the ligand which are responsible for the radiative transitions. Thus, the intensity of the emission diminishes with the increasing presence of the Co(II) cations in solution due to the commencing of the complexation process. As increasingly higher quantities of free ligand is complexed the emission intensity decreases. This behavior may be useful in such applications where Co(II) cations should be detected and quantitatively evaluated.

4. Conclusions

Three new complexes of Co^{2+}, Cd^{2+} and Rh^{3+} with 2 - (1H-1, 2, 4-triazol-3-yl) pyridine (Htzp) were obtained and studied. The compounds were characterized in the solid state by elemental analysis, XRD analysis, magnetic, conductivity and thermogravimetric measurements, DR and FTIR spectrophotometry. The experimental data show that the HTtzp acts as anionic bidentate ligand, tzp^-, and complexation reactions led to $[Co(tzp)_2]\cdot 1.5H_2O$, $[Cd(tzp)_2]$ and $[Rh(tzp)_3]\cdot H_2O$ compounds. The infrared, UV-Vis and P-XRD data indicate that tzp^- binds metal cations through nitrogen atom of pyridine and nitrogen 1 atom of triazole group. The thermogravimetric data confirm these bonding modes.

The absorption spectra suggest that the Co^{2+} and Cd^{2+} complexes are tetrahedral and Rh^{3+} complex adopt a distorted octahedral symmetry. In case of Co(II) complex, an interesting feature was noted, as the fluorescent emission intensity of the free ligand is dependent on the Co(II) solution content. Through complexation, the fluorescence is gradually quenched according to the Co(II) content, which may recommend it as a method of detection of Co(II) presence in waste water.

Aknowledgements
This work was supported by the strategic grant POSDRU/159/1.5/S/133652, co-financed by the European Social Fund within the Sectorial Operational Program Human Resources Development 2007 – 2013.

References

Alasalvar C., Soylu M.S., Ünver Y., Apaydın G., Ünlüer D., (2013), Spectroscopy studies, X-ray diffraction and DFT, HF calculations of 4-allyl-5-(thiophen-2-ylmethyl)-2H-1,2,4-triazol-3(4H)-one, *Journal of Molecular Structure,* **1033**, 243–252.

Bellagamba M., Bencivenni L., Gontrani L., Guidoni L., Sadun C., (2013), Tautomerism in liquid 1,2,3-triazole: a combined energy-dispersive X-Ray diffraction, molecular dynamics and FTIR study, *Chemical Physics*, **24**, 933-943.

Bladin J.A., (2006), Over dicyanphenylhydrazine and related compounds, *European Journal of Inorganic Chemistry,* **18**, 1544–1551.

Bortoluzzi M., Scrivanti A., Reolon A., Amadio E., Bertolasi V., (2013), Synthesis and characterization of novel gold(III) complexes with polydentate N-donor ligands based on the pyridine and triazole heterocycles, *Inorganic Chemistry Communications*, **33**, 82–85.

Chen S.C., Zhang Z.H., Zhou Y.S., Zhou W.Y., Li Y.Z., He M.Y., Chen Q., Du M., (2011), Alkali-metal-templated assemblies of new 3D Lead(II) tetrachloroterephthalate coordination frameworks, *Crystal Growth & Design*, **11**, 4190- 4197.

Crabtree R.H., (2001), *Introduction. The Organometallic Chemistry of the Transition Metals*, 3rd Ed., John Wiley, New York.

Ding B., Yi L., Gao H.L., Cheng P., Liao D.Z., Yan S.P., Jiang Z.H., (2005), 4-[3-(1,2,4-triazolyl)-1,2,4-triazole complexes of four-coordinated Cu(II) and six-coordinated Fe(II), *Inorganic Chemistry Communications,* **8**, 102-104.

Dong B.X., Gu X.J., Xu Q., (2010), Solvent effect on the construction of two microporous yttrium-organic frameworks with high thermostability via in situ ligand hydrolysis, *Dalton Transactions*, **39**, 5683-5687.

Haasnoot J.G., (2000), Mononuclear, oligonuclear and polynuclear metal coordination compounds with 1,2,4-triazoles derivates as ligands, *Coordination Chemistry Reviews*, **200–202**, 131–185.

Inkaya E., Dinçer M., Ekici Ö., Cukurovali A., (2013), 1-(3-Methyl-3-mesityl)-cyclobutyl-2-(5-pyridin-4-yl-2H-[1,2,4]triazol-3-ylsulfanyl)-ethanone: X-ray structure, spectroscopic characterizationand DFT studies, *Spectrochimica Acta Part A: Molecular and Biomolecular Spectroscopy,* **101**, 218–227.

Liu T.F., Lu J., Tian C., Coa M., Lin Z., Cao R., (2011), Porous anionic, cationic, and neutral metal-carboxylate frameworks constructed from flexible tetrapodal ligands: syntheses, structures, ion-exchanges, and magnetic properties, *Inorganic Chemistry*, **50**, 2264- 2271.

Meek S.T., Greathouse J.A., Allendorf M.D., (2011), Metal-organic frameworks: a rapidly growing class of versatile nanoporous materials, *Advanced Materials*, **23**, 249- 267.

Meunier-Piret J., Piret P., Putzeys J.P., Van Meerssche M., (1976), Cristalline structure of hexakis-(benzotriazolyl)-hexakis(allylamine)-trisnickel(II) with triphenylphosphine oxyde, *Acta Crystallographica*, **B32**, 714–717.

Mészáros S.K., Ivegeš E.Z., Leovac V.M., Vojinović Lj.S., Kovács A., Pokol G., Madarász J., Jaćimović Ž.K., (1998), Transition metal complexes with pyrazole-based ligands. Part 6: Synthesis, characterization and thermal decomposition of cadmium complexes with 3(5)-amino-5(3)-methylpyrazole, *Thermochimica Acta*, **316**, 79–85.

Nakamoto K., (1997), *Infrared and raman spectra of coordination compounds*, Part A, 5th Ed., John Wiley and Sons, New York.

Pardeshi S., Bobade V.D., (2011), Synthesis and biological evaluation of some novel triazol-3-ones as antimicrobial agents, *Bioorganic & Medicinal Chemistry Letters*, **21**, 6559–6562.

Potts K.T., (1961), The Chemistry of 1,2,4-Triazoles, Chemical Reviews, **61** , 87-127.

Reedijk J., Peerke I.M. van der List, Oldenbroek S.J.L., Lugthart E.N., Albada G.A. van, Gamez P., Haasnoot J.G., Teat S.J., Roubeau O., Mutikainen I., (2011), Coordination network solids based on Cu(II) coordination compounds with 1,4-bis-(1,2,4-triazol-1-yl)-butane as a flexible alkyl spacer ligand: Synthesis,characterization and X-ray structures, *Inorganica Chimica Acta*, **370,** 164–169.

Sasidharan N., Hariharanath B., Rajendran A.G., (2011), Thermal decomposition studies on energetic triazole derivatives, *Thermochimica Acta,* **520**, 139–144.

Shan G.G., Li H.B., Cao H.T., Sun H.Z., Zhu D.X., Su Z.M., (2013), Influence of alkyl chain lengths on the properties of iridium(III)-based piezochromic luminescent dyes with triazole-pyridine type ancillary ligands, *Dyes and Pigments,* **99**, 1082-1090.

Shang X., Han D., Li D., Wuc Z., (2013), Theoretical study of injection, transport, absorption and phosphorescence properties of a series of heteroleptic iridium(III) complexes in OLEDs, *Chemical Physics Letters*, **565** , 12–17.

Stock N., Biswas S., (2012), Synthesis of metal-organic frameworks (MOFs): routes to various MOF topologies, morphologies, and composites, *Chemical Reviews*, **112**, 933- 969.

Tabatabaee M., Tahriri M., Tahriri M., Ozawa Y., Neumüller B., Fujioka H., Toriumi K., (2012), Preparation, crystal structures, spectroscopic and thermal analyses of twoco-crystals of [M(H2O)6][M(dipic)2] and (atrH)2[M(dipic)2] (M = Zn, Ni,dipic = dipicolinate; atr = 3-amino-1H-1,2,4-triazole) with isostructural crystals system, *Polyhedron,* **33**, 336–340.

Yousif E., Haddad R., Ahmed A., (2013), Synthesis and characterization of transition metal complexes of 4-amino-5-pyridyl-4H-1,2,4-triazole-3-thiol, *Springer Plus*, **2**, 510.

Werner A., Stiasny E., (1899), Nitroderivates of Azo-, Azoxy- and Hydrazo-Benzols, *Berichte,* **32**, 3256–3282.

Wilson R.F., Wilson L.E., (1955), Preparation of Palladium(II) Chloride-1,2,3-Benzotriazole Coordination Compound, *Journal of the American Chemical Society*, **77**, 6204–6205.

Zhang J.P., Chen X.M., (2006), Crystal engineering of binary metal imidazolate and triazolate frameworks, *Chemical Communications*, **16**, 1689-1699.

Zhang R.Z., Zhang X.Z., (2013), Molecular structure, NMR parameters of N-(1,3,4-thiadiazol-2-yl)-1-[1-(6chloropyridin -3-yl) methyl]-5-methyl-1H-[1,2,3] triazol-4-carboxamide by density functional theory and *ab-initio* Hartree-Fock calculations, *Indian Journal of Pure & Applied Physics,* **51**, 164-173.